Proceedings of the ASME 2022
International Design Engineering Technical Conferences and
Computers and Information in Engineering Conference
IDETC/CIE2022
August 14-17, 2022, St. Louis, Missouri

DETC2022-90616

PARAMETRIC ANALYSIS OF NEGATIVE CAPACITANCE CIRCUIT FOR ENHANCED VIBRATION SUPPRESSION THROUGH PIEZOELECTRIC SHUNT

Ting Wang
Department of Mechanical Engineering
University of Connecticut
Storrs, CT 06269
Ting.2.wang@uconn.edu

J. Tang
Department of Mechanical Engineering
University of Connecticut
Storrs, CT 06269
jiong.tang@uconn.edu

ABSTRACT

Piezoelectric transducers are widely employed in vibration control and energy harvesting. The effective electro-mechanical coupling of a piezoelectric system is related to the inherent capacitance of the piezoelectric transducer. It is known that passive vibration suppression through piezoelectric LC shunt can be enhanced with the integration of negative capacitance which however requires a power supply. This research focuses on the parametric investigation of a self-sustainable negative capacitance where the piezoelectric transducer is concurrently used in both vibration suppression and energy harvesting through LC shunt. The basic idea is to utilize the energy harvesting functionality of the piezoelectric transducer to aid the usage of negative capacitance in terms of power supply. Specifically, the power consumption and circuitry performance with respect to negative capacitance circuit design is analyzed thoroughly. Indeed, the net power generation is the difference between available power in the shunt circuit and the power consumption of the negative capacitance circuit. There exists complex tradeoffs between net power generation and the vibration suppression performance when we use different resistance values in the negative capacitance circuit. It is demonstrated through correlated analytical simulation and experimental study that the proper selection of the resistance values in the negative capacitance circuit can result in vibration suppression enhancement as well as improved net power generation, leading to a self-sustainable negative capacitance scheme.

Keywords: piezoelectric transducer, vibration suppression, negative capacitance

1. INTRODUCTION

Piezoelectric transducers have been widely used in passive vibration suppression. Due to the electro-mechanical coupling of piezoelectric transducers, mechanical energy can be converted to electrical energy to be stored and/or dissipated in shunt circuits, resulting in the realization of vibration suppression [1]. A variety of efforts have been made to enhance the vibration suppression performance through mechanical designs [2] and circuitry tailoring [3]. Traditionally, the RL circuit, i.e., shunting with an inductor and a resistor, has been adopted which is analogous to tuned mass damper [4,5]. There have been studies focusing on reducing the negative effect of the inherent piezoelectric capacitance. Indeed, due to the existence of inherent capacitance, electric energy cannot be fully released into the piezoelectric shunt, leading to poor energy conversion. To overcome this issue, the usage of negative capacitance (NC) has been suggested [6-8] to offset the inherent capacitance for higher electro-mechanical coupling. The combination of resonant circuits and negative capacitances was formed for enhanced broadband vibration control [9], tunable vibration control [10], optimal performance [11], and multi-mode control [12].

Negative capacitance is realized based upon the Negative Impedance Converter (NIC) using operational amplifier (op-amp) [13]. An op-amp requires power supply. That is, an external power or battery is required for operating the vibration suppression with negative capacitance integration [14]. This largely restricts the application of negative capacitance in passive vibration suppression, because the employment of negative capacitance turns the system into semi-active [15]. Some studies have investigated the power consumption of op-amp [16]. There however doesn't seem to be a solution to address the power supply issue in passive vibration suppression enhancement. Intuitively, one may integrate vibration

suppression with energy harvesting capabilities of LC shunt, and seek a self-sustainable negative capacitance element by taking advantage of the power generation potential of the piezoelectric transducer under vibration. Nevertheless, there exists complicated parametric influence of NC circuit design with respect to op-amp power consumption, energy harvesting performance and actual vibration suppression performance. For example, more power may be harvested with large negative capacitance selection, but this also tends to diminish the vibration suppression enhancement. Moreover, different selections of NC circuit parameters, i.e., the resistance values involved in NC circuit, affect the overall robustness and stability of the circuitry dynamics [17,18].

The goal of this research is to explore and validate the parametric influence on the development of a self-sustainable NC element in an integrated vibration suppression enhancement and energy harvesting scheme through piezoelectric LC shunting. Section 2 provides system modeling details. In Section 3, the effects of the resistance in NC circuit to both net power and optional range of negative capacitance value is analyzed. Section 4 provides the experimental validation. The conclusions are summarized in Section 5.

2. SYSTEM-LEVEL MODELING AND ANALYSIS

2.1 Vibration suppression with negative capacitance

We consider a unimorph piezoelectric transducer with RL shunt. As shown in Fig.1, the host structure is a cantilever beam. In this research, we focus on the vibration suppression enhancement due to negative capacitance and the possibility of a self-sustainable scheme. The piezoelectric transducer is equivalent to a voltage source in series with an inherent capacitance. When an inductor and a resistor are added into the piezoelectric shunt, a LC piezoelectric resonant shunt is formed. The circuitry diagram is illustrated in Fig. 2, combing the LC resonant circuit with the negative capacitance which is realized through the usage of op-amp.

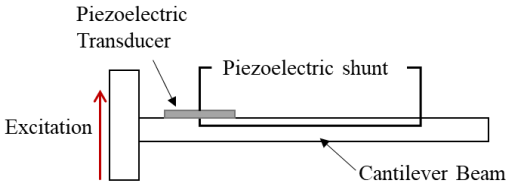

FIGURE 1: SKETCH OF THE INTEGRATED SYSTEM

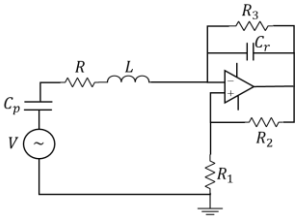

Figure 2: LC SHUNT WITH NEGATIVE CAPACITANCE

Based upon the simplified model [19], the system equations can be written as

$$\begin{cases} m\ddot{q} + c\dot{q} + kq + k_1 Q = F_m \\ L\ddot{Q} + R\dot{Q} + \hat{k}_2 Q + k_1 q = 0 \end{cases} \quad (1)$$

where q and Q are displacement and charge variables. m, k, and c are system equivalent mass, stiffness, and damping coefficients. k_1 represents the electro-mechanical coupling coefficient. F_m is the external excitation force. L and R are the inductance and resistance values. $\hat{k}_2$ coefficient is related to both the inherent capacitance of the piezoelectric transducer C_p and the introduced negative capacitance value C_n, i.e., $\hat{k}_2 = 1/C_p - 1/C_n$.

In this research, the resistance and inductance are selected to be the optimal values for the optimal vibration suppression performance [20], which are

$$L_{\text{opt}} = \frac{m\hat{k}_2}{k}, R_{\text{opt}} = \frac{k_1\sqrt{2m\hat{k}_2}}{k} \quad (2)$$

Under harmonic excitation, the transfer functions of displacement and charge in frequency-domain can be obtained as

$$\begin{cases} \frac{\bar{q}}{\bar{F}_m} = \frac{-\omega^2 L + i\omega R + \hat{k}_2}{(-\omega^2 L + i\omega R + \hat{k}_2)(-\omega^2 m + i\omega c + k) - k_1^2} \\ \frac{\bar{Q}}{\bar{F}_m} = \frac{-i\omega k_1}{(-\omega^2 L + i\omega R + \hat{k}_2)(-\omega^2 m + i\omega c + k) - k_1^2} \end{cases} \quad (3a, b)$$

Hereafter the overbar indicates the magnitude of the corresponding variable.

2.2 Self-sustainable negative capacitance

The negative capacitance circuit employs an op-amp which requires power. In this research we propose to use the same piezoelectric transducer for energy harvesting purpose. While the specific energy harvesting realization will be subject to future investigation, here we focus on the feasibility of self-sustainable negative capacitance, and investigate the power available in the shunt circuit. Such power can be utilized to charge a rechargeable battery in the system. When the power harvested is greater than the power consumed by the op-amp employed in the negative capacitance circuit, the negative capacitance becomes self-sustainable. In energy harvesting research, commonly a resistor load is employed to quantify the energy harvesting capability. In order to ensure the optimal vibration control performance, the resistor load in this research is set as the optimal resistance shown in Eq. (2). The transfer function of the available power from the resistor element in the shunt versus the base excitation can be expressed as

$$\frac{\bar{P}_s}{\bar{F}_m^2} = \frac{(i\omega\bar{Q})^2 \cdot R_{\text{opt}}}{\bar{F}_m^2} \quad (4)$$

or

$$\frac{\bar{P}_s}{\bar{F}_m^2} = \frac{\omega^2 k_1^3 \sqrt{2m\hat{k}_2}}{k\left[(-\omega^2 L + i\omega R + \hat{k}_2)(-\omega^2 m + i\omega c + k) - k_1^2\right]^2} \quad (5)$$

According to Fig. 2, the negative capacitance value can be expressed as

$$-C_n = -rC_r = -\frac{R_2}{R_1} C_r \quad (6)$$

where C_r is the reference capacitance value, and C_n is the negative capacitance value. R_1 and R_2 are two resistances to determine the magnification r. To separate variable r from variable C_n for simplicity, here we set $R_2 = R_1$. Thus $r = 1$

and $C_n = C_r$. Usually, a relatively large resistance is selected for R_3, e.g., $R_3 = 10M\Omega$ in this research. The power consumption of the op-amp can be obtained based upon the output voltage and output current of the op-amp as

$$\frac{\bar{P}_{\text{op-amp}}}{\bar{F}_m^2} = \frac{\bar{V}_{\text{out}}}{\bar{F}_m} \cdot \frac{\bar{I}_{\text{out}}}{\bar{F}_m} \tag{7}$$

The op-amp is assumed to be ideal, i.e., there is no current going through the two input terminals of the op-amp and there is no voltage difference between two input terminals of the op-amp. Based upon the voltage divider rule and $R_2 = R_1$, the output voltage of op-amp is twice the input voltage of op-amp. Similarly, based upon the current division, the output current of the op-amp is the sum of the current going through the upper and the lower branch. At the inverting input terminal, with the ideal assumption of no current going into the op-amp, the current in the main shunt is the negative value of output current of the upper branch.

Combining the equations of output voltage and current with that of charge generated in the main shunt (Eq. (3b)), we can derive the power consumption of op-amp as

$$\frac{\bar{P}_{\text{op-amp}}}{\bar{F}_m^2} = \frac{2k_1^2(1+i\omega R_1 C_n)}{(R_1 C_n)^2\left[(-\omega^2 L + i\omega R + \hat{k}_2)(-\omega^2 m + i\omega c + k) - k_1^2\right]^2} \tag{8}$$

The net power for self-sustainability can be obtained by calculating the magnitude difference between the available power in Eq. (5) and the power consumption of op-amp in Eq. (8). The final magnitude of the net power transfer function can be expressed as

$$\left|\frac{\bar{P}_{\text{net}}}{\bar{F}_m^2}\right| = \left|\frac{\bar{P}_s}{\bar{F}_m^2}\right| - \left|\frac{\bar{P}_{\text{op-amp}}}{\bar{F}_m^2}\right| \tag{9}$$

A self-sustainable negative capacitance can be achieved by ensuring positive net power, i.e., equation (9) should be positive. Then the optional negative capacitance range can be obtained from solving the following inequality:

$$C_n^4 - C_p C_n^3 - \frac{2kC_p}{k_1^2} C_n^2 - \frac{2mC_p}{k_1^2 R_1^2} > 0 \tag{10}$$

We can find the critical negative capacitance value from the above equation by setting the net power to be zero. Therefore, the self-sustainable vibration suppression enhancement system with negative capacitance integration requires the negative capacitance value to be larger than the critical negative capacitance value.

3. PARAMETRIC ANALYSIS OF NC CIRCUIT

From Eq. (9) and Eq. (10), it is noted that both net power magnitude and critical negative capacitance value are closely related to the resistance value R_1. Indeed, the resistance value R_1 has potential in affecting both net power for higher self-sustainability and optional value of negative capacitance for enhanced vibration suppression. In this section, the influence of the resistance value R_1 is analyzed.

3.1 Effect to net power

The net power magnitude shown in Eq. (9) is related to the available power (Eq. (5)) and the power consumption of op-amp (Eq. (8)). As shown in Eq. (5), the available power only depends on the negative capacitance value. As mentioned in Section 2.2, we separate the negative capacitance value C_n from the negative capacitance circuit resistance selection by setting $R_2 = R_1$. Therefore, the available power of the optimal resistance in Eq. (5) is independent from the specific NC circuit parametric selection. On the other hand, the power consumption of op-amp shown in Eq. (8) depends on not only the negative capacitance value, but also the resistance R_1 of the NC circuit. As a result, the net power is related to resistance R_1. When LC resonant circuit is employed, the system vibration suppression performance is mainly reflected by the plateau-like responses near the resonant frequency. To explore the relationship between the net power magnitude and the resistance R_1, we focus on the peak net power amplitude at the resonant frequency. As illustrated in Fig. 3, when the resistance R_1 increases, the net power also increases from negative value to positive value. Under a very large negative capacitance value 1000 nF (compared to the piezoelectric inherent capacitance 11.42 nF), the positive net power is always ensured. Nevertheless, under that negative capacitance selection, the enhancement of vibration suppression is rather small, as mentioned in Section 2.1. Under a smaller negative capacitance 500 nF, larger resistance R_1 is required to ensure the positive net power.

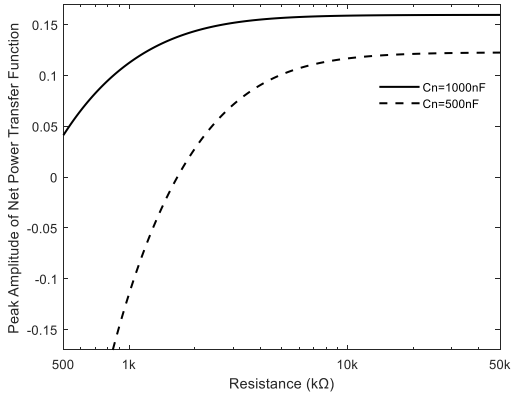

FIGURE 3: PEAK MAGNITUDE OF NET POWER VS THE RESISTANCE EMPLOYED IN NEGATIVE CAPACITANCE CIRCUIT

3.2 Effect to critical negative capacitance value

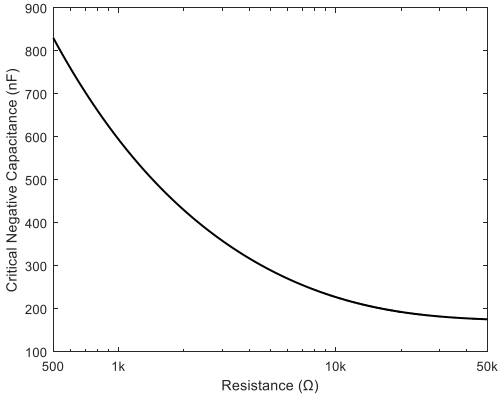

FIGURE 4: CRITICAL CAPACITANCE VALUE VS THE RESISTANCE EMPLOYED IN NEGATIVE CAPACITANCE CIRCUIT

From Eq. (10), one may see that the critical negative capacitance is closely related to the resistance value R_1, which is reported in Fig. 4. It can be observed that the critical negative capacitance value is very large (larger than 800 nF) under small resistance value $R_1 = 500\Omega$. However, in such situation, the vibration suppression enhancement becomes very limited. By increasing the resistance value R_1, the critical negative capacitance value can be reduced, i.e., the feasible range of negative capacitance value is enlarged, and a smaller negative capacitance value can be selected for better vibration suppression enhancement performance.

3.3 Vibration suppression enhancement with self-sustainable negative capacitance

The goal of this research is to enhance the vibration suppression performance through the usage of self-sustainable negative capacitance. That is, we want to reduce the negative capacitance value for higher vibration suppression, but at the same time, the net power needs to remain to be positive for system self-sustainability. As analyzed in Section 3.1 and Section 3.2, it appears that larger resistance R_1 is favorable for both increasing the net power (Fig. 3) and decreasing the critical negative capacitance value (Fig. 4). It means that with larger resistance R_1, smaller negative capacitance can be used for greater vibration suppression, and the net power can also be larger for higher self-sustainability. Here we further investigate such phenomena and come up with the tuning strategy.

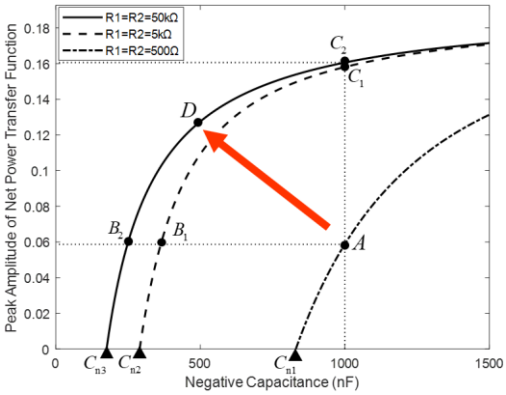

FIGURE 5: NET POWER MAGNITUDES VS NEGATIVE CAPACITANCE UNDER DIFFERENT NC RESISTANCES

According to the net power transfer function (Eq. (9)), the net power is closely correlated with two parameters, the negative capacitance C_n and the NC resistance R_1. Here we focus on the parametric influence at the resonant frequency which is representative for performance assessment. Under different R_1 values, the peak amplitude of the net power transfer function at resonant frequency versus negative capacitance is plotted in Fig. 5. Three different R_1 values are considered, 500Ω, $5\text{k}\Omega$, and $50\text{k}\Omega$. Under each R_1 value, the net power increases with the increase of the negative capacitance value. The intersection of each curve and the x-axis is the critical negative capacitance value (Eq. (10)). For achieving positive net power, the negative capacitance value needs to be selected above this critical negative capacitance. Therefore, if we want to use smaller negative capacitance value and still maintain the positive net power, we need to reduce the critical negative capacitance value.

As can be seen in Fig. 5, the curve of net power versus negative capacitance with large resistance R_1 generally is located at the left side. When the resistance R_1 increases from 500Ω to $5\text{k}\Omega$ and then to $50\text{k}\Omega$, the intersection of the respective curve and the x-axis decreases from C_{n1} to C_{n2} to C_{n3}. This means the critical negative capacitance decreases when the NC resistance R_1 increases. In other words, if we use larger resistance R_1, we can have smaller negative capacitance value to maintain positive net power, and this smaller negative capacitance value can yield greater vibration suppression performance. For example, when the resistance R_1 is selected to be small as $500\ \Omega$, if 0.06 peak net power magnitude is required for system self-sustainability, the negative capacitance value needs to be 1000 nF (point A in Fig. 5). This value however is too large for producing meaningful vibration suppression enhancement. However, when the resistance R_1 is selected to be a larger value $5\ \text{k}\Omega$, a smaller negative capacitance value 360.5 nF (point B_1 in Fig. 5) can result in the same 0.06 peak net power magnitude and the vibration suppression can be enhanced much more significantly. When the resistance R_1 is further increased to $50\ \text{k}\Omega$, a further smaller negative capacitance value 242 nF (point B_2 in Fig. 5) can maintain the same 0.06 peak net power magnitude and the vibration suppression can be further enhanced. We can follow this tuning criterion when the net power value is fixed to a certain positive value, and seek for maximum vibration suppression performance enhancement.

Meanwhile, if the vibration suppression performance is fixed at certain expected value, the negative capacitance value is fixed. Then the main focus will be to maximize the net power by using a larger resistance R_1. For example, under the same negative capacitance value 1000 nF (point A in Fig. 5), when the resistance R_1 increases from $500\ \Omega$ to $5\ \text{k}\Omega$ and then to $50\ \text{k}\Omega$, the peak net power magnitude can increase from 0.06 to 0.15 and then to 0.16, which corresponds to the trajectory from point A to C_1 and then to C_2. Apparently, the vibration suppression enhancement and the self-sustainability can be increased simultaneously. As shown in Fig. 5, if we pick point D between the line segment B_2C_2 with much larger resistance $R_1 = 50\text{k}\Omega$, the abscissa value of point D is smaller than 1000nF at point A with small resistance $R_1 = 500\Omega$, which means the negative capacitance value is reduced so vibration suppression is enhanced. At the same time, the ordinate value of the point D is larger than 0.06 at point A with small resistance $R_1 = 500\Omega$, which means the net power also increases. As a result, by using larger enough resistance R_1 like $50\text{k}\Omega$ and selecting the negative capacitance value between the line segment B_2C_2, both vibration suppression and system self-sustainability are be enhanced. Of course, as illustrated in Fig. 5, when the resistance R_1 increases further, the benefit becomes smaller.

4. RESULTS AND DISCUSSION

This section presents the experimental results for validation. The experimental setup is shown in Fig. 6. The cantilever beam (6061 Al) bonded with a piezoelectric patch (APC 850) is mounted on a shaker (APS 400). A controller (VR9500) is utilized to drive the power amplifier (APS 145) for shaker operation. An accelerometer (PCB 352C04) is glued on the shaker to make sure constant excitation acceleration. The circuitry responses are measured using an oscilloscope (Keysight DSOX1204G). The vibration responses are measured using a scanning laser vibrometer (Polytec PSV-500).

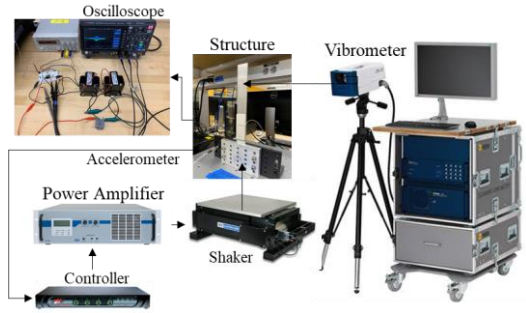

Figure 6: EXPERIMENTAL SETUP

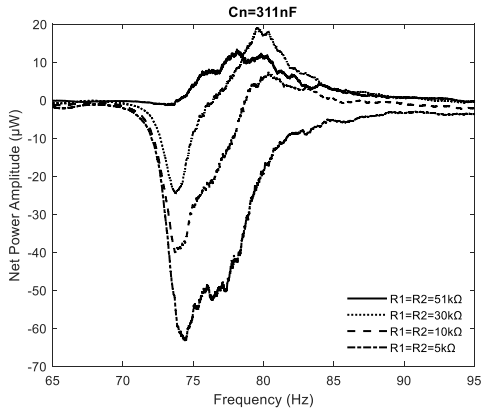

FIGURE 7: NET POWER INCREASE BY USING LARGER RESISTANCE IN NEGATIVE CAPACITANCE CIRCUIT

The beneficial effect of increasing resistance R_1 of the NC circuit on net power generation can be observed in Fig. 7. With the same 311 nF NC value, when the resistance R_1 is increased, the frequency responses of the net power indeed change from completely negative, to partially positive, and then to entirely positive within the frequency range of interest. This matches very well to the predicted relationship between net power and resistance R_1 shown in Fig. 3. Also, the results in Fig. 7 validate the trend moving up from point A to B_1 and then to B_2. That is, with the same negative capacitance value, self-sustainability can be enhanced by increasing the resistance R_1 of the negative capacitance circuit.

To examine the simultaneous enhancements of both vibration suppression and self-sustainability (i.e., the direction of the red arrow in Fig. 5), a large negative capacitance value (954 nF) with a small NC resistance $R_1 = 511\ \Omega$ is selected which corresponds to approximately point A in Fig. 5. Another much smaller negative capacitance value (362 nF) with very large resistance $R_1 = 51\text{k}\Omega$ is selected to reflect the simultaneous enhancement happened at point D. The net power results under these two conditions are shown in Fig. 8. Compared to the large negative capacitance value case (954 nF), the smaller negative capacitance value (362 nF) achieves a significant increase in net power magnitude, near five times, due to the application of large resistance $R_1 = 51\text{k}\Omega$.

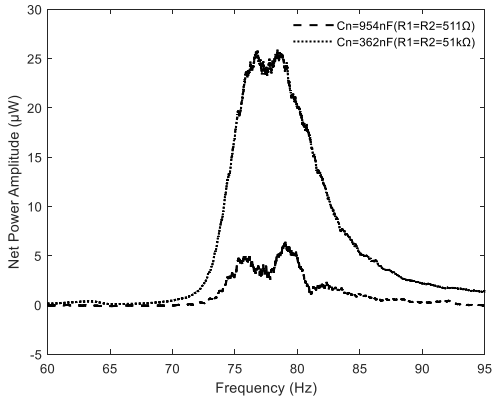

FIGURE 8: NET POWER PERFORMANCE UNDER DIFFERENT NEGATIVE CAPACITANCE VALUES AND R_1 VALUES

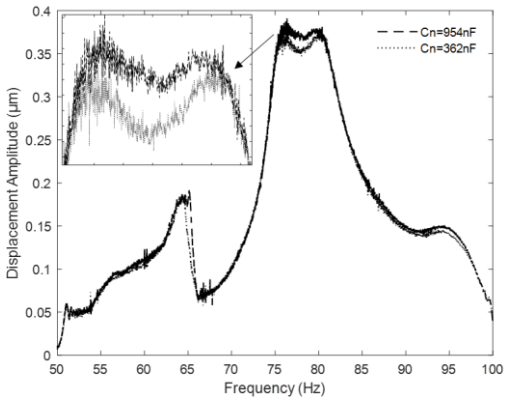

FIGURE 9: VIBRATION SUPPRESSION PERFORMANCE UNDER DIFFERENT NEGATIVE CAPACITANCE VALUES AND R_1 VALUES

The vibration suppression performance comparison between under the aforementioned two negative capacitance values, 954 nF and 362 nF, are shown in Fig. 9. When the negative capacitance value decreases from 954 nF to 362 nF, further vibration suppression can be observed around the resonant frequency, which is about 4.08%. The amount of enhancement depends on the negative capacitance value. When a very large resistance $R_1 = 51\text{k}\Omega$ is employed in the negative capacitance circuit, the critical negative capacitance value decreases to as small as 175.76 nF. The negative capacitance value can be selected even smaller than 362 nF for greater vibration suppression enhancement, as long as the negative capacitance value is greater than 175.76 nF.

The experimental results shown in in Fig. 8 and Fig. 9 confirm that simultaneous enhancements of both vibration suppression and net power can be achieved by employing large resistance R_1 in the negative capacitance circuit. The negative capacitance can be selected freely within the proposed selection range. Smaller negative capacitance within the selection range tends to enhance the vibration suppression more, which corresponds to the area above the red arrow in Fig. 5. On the other hand, larger negative capacitance within the selection range tends to enhance the net power more, which corresponds to the area blow the red arrow in Fig. 5.

5. CONCLUSION

In this research, based on power consumption analysis, we conduct a parametric investigation on a self-sustainable negative capacitance scheme to enhance vibration suppression using LC shunt. In this scheme, the piezoelectric shunt is used concurrently for energy harvesting. It is found that a properly designed negative capacitance circuit can enhance vibration suppression performance and at the same time can be self-sustainable when integrated with energy harvesting. Larger resistance used in the negative capacitance circuit can benefit the net power in the integrated system.

ACKNOWLEDGEMENTS

This research is supported in part by the DOT Transportation Infrastructure Durability Center at the University of Maine under grant 69A3551847101, and in part by NSF under grant CMMI – 1825324.

REFERENCES

[1] Zhao, L., 2016, "Passive vibration control based on embedded acoustic black holes," *ASME J. Vib. Acoust.*, 138(4), p. 041002.

[2] Zhang, F., Liu, J. and Tian, J., 2021, "Analysis of the Vibration Suppression of Double-Beam System via Nonlinear Switching Piezoelectric Network," *Machines*, 9(6), p.115.

[3] Yan, B., Zhou, S. and Litak, G., 2018, "Nonlinear analysis of the tristable energy harvester with a resonant circuit for performance enhancement," *Int. J. Bifurc. Chaos*, 28(07), p.1850092.

[4] Yamada, K., 2017, "Complete passive vibration suppression using multi-layered piezoelectric element, inductor, and resistor," *J. Sound Vib.*, 387, pp.16-35.

[5] Kozlowski, M. V., Cole, D. G., and Clark, R. L., 2011, "A comprehensive study of the RL series resonant shunted piezoelectric: a feedback controls perspective," *ASME J. Vib. Acoust.*, 133(1), p. 011012.

[6] Zhao, J., Wang, X., and Tang, J., 2011, "Damping reduction in structures using piezoelectric circuitry with negative resistance," *ASME J. Vib. Acoust.*, 133(4), p. 041009.

[7] Zhang, F., Liu, J., and Tian, J., 2021, "Analysis of the Vibration Suppression of Double-Beam System via Nonlinear Switching Piezoelectric Network," *Machines*, 9(6), p.115.

[8] Billon, K., Montcoudiol, N., Aubry, A., Pascual, R., Mosca, F., Jean, F., Pezerat, C., Bricault, C., Chesné, S., 2020, "Vibration isolation and damping using a piezoelectric flextensional suspension with a negative capacitance shunt," *Mech. Syst. Signal Process.*, 140, p. 106696.

[9] Berardengo, M., Manzoni, S., Vanali, M., and Bonsignori, R., 2021, "Enhancement of the broadband vibration attenuation of a resistive piezoelectric shunt," *J. Intell. Mater. Syst. Struct.*, 32(18-19), pp. 2174-2189.

[10] Berardengo, M., Manzoni, S., Thomas, O., and Vanali, M., 2021, "Guidelines for the layout and tuning of piezoelectric resonant shunt with negative capacitances in terms of dynamic compliance, mobility and accelerance," *J. Intell. Mater. Syst. Struct.*, 32(17), pp. 2092-2107.

[11] Berardengo, M., Manzoni, S., Thomas, O., and Vanali, M., 2018, "Piezoelectric resonant shunt enhancement by negative capacitances: Optimisation, performance and resonance cancellation," *J. Intell. Mater. Syst. Struct.*, 29(12), pp. 2581-2606.

[12] Berardengo, M., Thomas, O., Giraud-Audine, C., and Manzoni, S., 2017, "Improved shunt damping with two negative capacitances: an efficient alternative to resonant shunt," *J. Intell. Mater. Syst. Struct.*, 28(16), p. 2222-2238.

[13] Turco, E., Gardonio, P., Petrella, R., and Dal Bo, L., 2020, "Modular Vibration Control Unit Formed by an Electromagnetic Proof-Mass Transducer and Sweeping Resistive–Inductive Shunt," *ASME J. Vib. Acoust.*, 142(6), p. 061005.

[14] Burnett, J. K., Choi, Y. T., Li, H., Wereley, N. M., Miller, R., and Shim, J. K., 2021, "Vibration Suppression of a Composite Prosthetic Foot Using Piezoelectric Shunt Damping: Implication to Vibration-Induced Cumulative Trauma," *IEEE Trans. Biomed. Eng.*, 68(9), pp. 2741-2751.

[15] Paknejad, A., Zhao, G., Chesné, S., Deraemaeker, A., and Collette, C., 2021, "Hybrid electromagnetic shunt damper for vibration control," *ASME J. Vib. Acoust.*, 143(2), p. 021010.

[16] Qureshi, E. M., Shen, X., and Chang, L., 2015, "Power output and efficiency of a negative capacitance and inductance shunt for structural vibration control under broadband excitation," *Int. J. Aeronaut. Space Sci.*, 16(2), pp. 223-246.

[17] Berardengo, M., Manzoni, S., Thomas, O., Giraud-Audine, C., Drago, L., Marelli, S., and Vanali, M., 2021, "The reduction of operational amplifier electrical outputs to improve piezoelectric shunts with negative capacitance," *J. Sound Vib.*, 506, p. 116163.

[18] Manzoni, S., Moschini, S., Redaelli, M., and Vanali, M., 2012, "Vibration attenuation by means of piezoelectric transducer shunted to synthetic negative capacitance," *J. Sound Vib.*, 331(21), pp. 4644-4657.

[19] Xu, J., and Tang, J., 2015, "Linear stiffness compensation using magnetic effect to improve electro-mechanical coupling for piezoelectric energy harvesting," *Sens. Actuator A Phys.*, 235, pp. 80-94.

[20] Tang, J., and Wang, K. W., 1999, "Vibration Control of Rotationally Periodic Structures Using Passive Piezoelectric Shunt Networks and Active Compensation," *ASME J. Vibr. Acoust.*, 121(3), pp. 379–390.

